Synthesis and Structural Characterization of Several Ruthenium Porphyrin Nitrosyl Complexes

Katrina M. Miranda,[1] Xianhui Bu, Ivan Lorković, and Peter C. Ford*

Department of Chemistry, University of California, Santa Barbara, California 93106

Received January 17, 1997[⊗]

The synthesis, X-ray crystal structures, and some spectroscopic and chemical properties of the nitrosylruthenium(II) porphyrin complexes Ru(TPP)(NO)(ONO), Ru(TPP)(NO)(OH), Ru(OEP)(NO)(ONO), and Ru(OEP)(NO)(OH) (TPP = tetraphenylporphyrinato dianion; OEP = octaethylporphyrinato dianion) derived from the analogous Ru(II) carbonyl complexes are reported. Also described are experiments which quantitatively demonstrate that N_2O is formed as a product of the synthesis scheme and that NO serves as the principal oxidant in the transformation of N(II) to N(III). The two TPP complexes are isostructural and consist of columns of molecules stacked along the *c* axis. The two OEP complexes are also isostructural and can be considered as layers of OEP complexes stacked along the *b* axis with solvent molecules situated at the cavities between layers. The nitrite ions are coordinated in a unidentate fashion through the oxygen atom. Crystal data for Ru(TPP)(NO)(ONO) (**1**): M = 789.79, space group $I4/m$ (No. 87), a = 13.6529(6) Å, c = 9.7904(5) Å, V = 1825.0(2) Å^3, Z = 2, ρ = 1.437 g cm^{-3}, purple bipyramid, $2\theta_{max}$ = 50.0°, $R(F)$ = 4.87% for 86 parameters and 838 reflections with $I > 2\sigma(I)$. Crystal data for Ru(TPP)(NO)(OH) (**2**): M = 760.79, space group $I4/m$ (No. 87), a = 13.5423(4) Å, c = 9.7150(4) Å, V = 1781.7(1) Å^3, Z = 2, ρ = 1.418 g cm^{-3}, dark red plate, $2\theta_{max}$ = 50.0°, $R(F)$ = 3.92% for 83 parameters and 811 reflections with $I > 2\sigma(I)$. Crystal data for Ru(OEP)(NO)(ONO)·CH_2Cl_2 (**3**): M = 794.77, space group $P2_1$ (No. 4), a = 10.7687(2) Å, b = 21.0320(2) Å, c = 8.5936(2) Å, β = 102.683(1)°, V = 1898.85(6) Å^3, Z = 2, ρ = 1.390 g cm^{-3}, black plate, $2\theta_{max}$ = 50.0°, $R(F)$ = 6.23% for 453 parameters and 4702 reflections with $I > 2\sigma(I)$. Crystal data for Ru(OEP)(NO)(OH)·C_2H_5OH (**4**): M = 726.91, space group $P2_1$ (No. 4), a = 10.8474(7) Å, b = 21.002(1) Å, c = 8.3646(5) Å, β = 103.571(1)°, V = 1852.4(2) Å^3, Z = 2, ρ = 1.303 g cm^{-3}, brown plate, $2\theta_{max}$ = 45.0°, $R(F)$ = 6.74% for 421 parameters and 3527 reflections with $I > 2\sigma(I)$.

Introduction

The discoveries that nitric oxide serves important roles in mammalian bioregulation of functions such as vasodilation, bronchodilation, and neurotransmission and is an important constituent in immune response to infection have stimulated intense interest in the chemistry and biochemistry of NO and derivatives such as metal nitrosyl complexes.[2] Also of interest are precursor compounds that can serve to deliver NO to biological targets on demand.[3] One strategy would be to employ a precursor that displays relatively low thermal reactivity but is photochemically active to give NO when subjected to electronic excitation. This proposition has been the stimulus of investigations by members of this laboratory into the thermal and photochemical reactivities of several different types of metal nitrosyl complexes,[4−7] including certain nitrosyl metalloporphyrin complexes.

In the course of these studies, it was found that nitrosyl porphyrin complexes of the first-row transition metals prepared in this laboratory[1a] proved too labile, too reactive with dioxygen, or both to be promising for practical applications in photochemical NO delivery to specific targets in biological organisms. As a consequence, our attention turned to the preparation of ruthenium analogs, which were anticipated to be more stable. The present article describes the synthesis from the carbonyl analogs Ru(P)(CO), spectroscopic characterizations, and the structures of several nitrosylruthenium complexes of tetraphenylporphyrinate(2−) (TPP) and octaethylporphyrinate(2−) (OEP). Also described are studies to elucidate the stoichiometry of the reactions involved. Photochemical properties of these compounds will be described elsewhere.[8]

Notably, when these studies were initiated, the literature of ruthenium nitrosyl porphyrin complexes was sparse,[9−11] and the structures of such Ru(P)(NO) species had not been reported. In the interim, however, the syntheses and crystal structures of several ruthenium nitrosyl porphyrins have been published,[12−14]

[⊗] Abstract published in *Advance ACS Abstracts,* September 1, 1997.

(1) (a) Taken in part from the Ph.D. dissertation of K.M., University of California, Santa Barbara, 1996. (b) Reported in part at the 207th National Meeting of the American Chemical Society, San Diego, CA, March 1994; see Abstract INORG 313.
(2) (a) Palmer, R. M. J.; Ferrige, A. G.; Moncada, S. *Nature* **1987**, *327*, 524−526. (b) Ignarro, L. J.; Buga, G. M.; Wood, K. S.; Byrns, R. E.; Chaudhuri, G. *Proc. Natl. Acad. Sci. U.S.A.* **1987**, *84*, 9265−9269. (c) Hibbs, J. B., Jr.; Taintor, R. R.; Vavrin, Z. *Science* **1987**, *235*, 473−476. (d) Furchgott, R. F.; Vanhoute, P. M. *FASEB J.* **1989**, *3*, 2007−2018. (e) Moncada, S.; Palmer, R. M. J.; Higgs, E. A. *Pharmacol. Rev.* **1991**, *43*, 109−142. (f) Feldman, P. L.; Griffith, O. W.; Stuehr, D. J. *Chem. Eng. News* **1993**, *71* (10) 26−38. (g) Wink, D. A.; Hanbauer, I.; Grisham, M. B.; Laval, F.; Nims, R. W.; Laval, J.; Cook, J.; Pacelli, R.; Liebmann, J.; Krishna, M.; Ford, P. C.; Mitchell, J. B. *Curr. Top. Cell. Regul.* **1996**, *34*, 159−187. (h) Feelish, M., Stamler, J. S., Eds. *Methods in Nitric Oxide Research*; John Wiley and Sons: Chichester, England, 1996; see also references therein.
(3) Feelish, M.; Stamler, J. S. In ref 2h, Chapter 7, pp 71−113.
(4) Hoshino, M.; Ozawa, K.; Seki, H.; Ford, P. C. *J. Am. Chem. Soc.* **1993**, *115*, 9568−9575.
(5) Tran, D.; Ford, P. C. *Inorg. Chem.* **1996**, *35*, 2411−2412.
(6) Hoshino, M.; Maeda, M.; Konishi, R.; Seki, H.; Ford, P. C. *J. Am. Chem. Soc.* **1996**, *118*, 5702−5707.
(7) Bourassa, J.; DeGraff, W.; Kudo, S.; Wink, D. A.; Mitchell, J. B.; Ford, P. C. *J. Am. Chem. Soc.* **1997**, *119*, 2853−2860.
(8) Miranda, K. M.; Lee, B.; Lorkovic, I.; Ford, P. Manuscript in preparation
(9) Srivastava, T. S.; Hoffman, T.; Tsutsui, M. *J. Am. Chem. Soc.* **1972**, *94*, 1385−1386.
(10) Antipas, A.; Buchler, J. W.; Gouterman, M.; Smith, P. D. *J. Am. Chem. Soc.* **1978**, *100*, 3015−3024.
(11) Massoudipour, M.; Pandey, K. K. *Inorg. Chim. Acta* **1989**, *160*, 115−118.

S0020-1669(97)00065-7 CCC: $14.00

including one of the species, Ru(TPP)(NO)(ONO), described in the present report.[12]

Experimental Section

Materials and Procedures. Reagent grade methylene chloride for synthesis and recrystallization was distilled from CaH_2 under N_2 directly before use. Chlorobenzene was passed through a neutral activated alumina column and stored over activated 4 Å molecular sieves. Column chromatography was performed on alumina (neutral activity I; Sigma) or silica (70−230 mesh; Aldrich). Ruthenium dodecacarbonyl (Strem Chemicals) and *meso*-tetraphenylporphine (Aldrich) were used as received. Ru(OEP)(CO) was obtained from Midcentury (Posen, IL) and as a gift from Dr. Mikio Hoshino of the Institute of Chemical and Physical Research (RIKEN), Wako-shi, Japan. The TPP analog Ru(TPP)(CO) was prepared by the literature method.[15]

Both samples of Ru(OEP)(CO) were subjected to column chromatography, on silica using CH_2Cl_2 as the eluent, to remove free-base (H_2OEP) impurities before use in synthesis. A single, streaked band was observed. Illumination with a hand-held fluorescent lamp indicated that H_2OEP eluted at the forefront of this band, so this strongly fluorescent portion was discarded. Several cycles were required to obtain pure free-base product as indicated by analytical thin-layer chromatography on silica ($60F_{254}$ on glass; Merck) with CH_2Cl_2. After this procedure, recrystallization was accomplished from 3:1 CH_2Cl_2/EtOH. Unreacted free base was removed from Ru(TPP)(CO)(EtOH) by column chromatography on alumina with CH_2Cl_2 as the eluent. The free base H_2TPP eluted as a red fluorescent band, while Ru(TPP)(CO) remained on the column. Product recovery was then effected by the addition of 2% 2-propanol in CH_2Cl_2. Recrystallization was accomplished in air by the slow evaporation of a 3:1 CH_2Cl_2/EtOH solvent mixture to give Ru(TPP)(CO)(EtOH). For both OEP and TPP derivatives, the weakly bound EtOH ligand ($K \sim 10^3$ M^{-1} in CH_2Cl_2) may be removed by dissolving the complex in CH_2Cl_2 and isolating again.

All syntheses of nitrosyl compounds were performed under chromatographic grade argon, which had been passed through an indicating oxygen trap (Chromatograph Research Supplies). NO (99.0% purity; Matheson) was purified of higher nitrogen oxides by passage through a stainless steel column containing Ascarite II (NaOH on a silicate carrier; Thomas Scientific). Deaeration of solvents was accomplished by entraining with argon for a minimum of 1 min/mL.

Instrumentation. Electronic absorption spectra were measured in 0.0202 cm CaF_2 and 0.2 and 1 cm quartz cells on Hewlett-Packard 8452A diode array and Cary 118 (OLIS digital upgrade) spectrophotometers. Infrared spectra of solid samples in a KBr matrix and of dichloromethane solutions were recorded with a Bio-Rad FTS-60 FTIR spectrophotometer. Gas chromatography measurements were made at 140 °C on a Hewlett Packard 5830A gas chromatograph equipped with a 12 ft Porapak Q (80−100 mesh) column with a TC detector and 10% H_2 in He as carrier gas (30 mL/min). NMR spectra were obtained on Varian 200, 400, and 500 MHz spectrometers in $CDCl_3$ ($CHCl_3$ at 7.260 ppm). FAB mass spectra (xenon atom bombardment of a 3-nitrobenzyl alcohol matrix) were obtained on a VG 70E double-focusing mass spectrometer.

Synthesis of Ru(TPP)(NO)(ONO) (1) and Ru(TPP)(NO)(OH) (2). A red suspension of Ru(TPP)(CO)(EtOH) (200 mg, 0.254 mmol) in deaerated CH_2Cl_2 (60 mL) was entrained with NO (40 min), during which all solids dissolved to form a deep red solution. After solvent removal with a stream of argon, the product was redissolved in minimal CH_2Cl_2, and the solution was loaded onto an alumina column. Elution with CH_2Cl_2 gave **1** as an olive green band on the column and a wine-colored solution. Elution with 2% EtOH/CH_2Cl_2 freed **2** from the column as a concise red band. Lustrous purple crystals of **1** (121 mg, 56% yield) were recovered by slow evaporation of CH_2Cl_2 in the dark. Mauve crystalline **2** (76 mg, 38% yield) was collected after addition of EtOH (30% v/v) to the eluted solution. Spectral data for **1**: UV/visible in CH_2Cl_2 (λ_{max}, nm (ϵ, $M^{-1}cm^{-1}$)) 333 (2.1×10^4), 410 (2.1×10^5, Soret), 564 (1.03×10^4), 608^{sh} (4.2×10^3); IR (KBr; cm^{-1}) 1854 (vs), 1522 (s), 930 (m); ^{1}H-NMR ($CDCl_3$; δ, ppm) 9.00 (8H, s, pyrrole β), 8.28 (4H, dm, $J = 6.8$ Hz, *ortho*), 8.20 (4H, dm, $J = 6.8$ Hz, *ortho*), 7.70 (12H, m, *meta*, *para*); FAB-MS (*m/z*) 744 (100, Ru(TPP)$(NO)^+$), 714 (50, Ru$(TPP)^+$). Spectral data for **2**: UV/visible in CH_2Cl_2 (λ_{max}, nm (ϵ, M^{-1} cm^{-1})) 320 (2.0×10^4), 410 (1.4×10^5, Soret), 428^{sh}, 556 (1.9×10^4), 592 (6.8×10^3); IR (KBr; cm^{-1}) 1827 (vs), 1817^{sh}; ^{1}H-NMR ($CDCl_3$; δ, ppm) 8.98 (8H, s, pyrrole β), 8.28 (8H, m, *ortho*), 7.80 (12H, m, *meta*, *para*) (hydroxo proton resonance not observed); MS (*m/z*) 744 (100, Ru(TPP)$(NO)^+$), 714 (63, Ru$(TPP)^+$). Optical spectra of **1** and **2** are included as figures in the Supporting Information.

Ru(OEP)(NO)(ONO) (3) and Ru(OEP)(NO)(OH) (4). The OEP analogs of the TPP complexes **1** and **2** were prepared from Ru(OEP)(CO)(EtOH) using the procedure described above except that NO entrainment of the orange solution was maintained for only 3 min. The material isolated from the second red band obtained from chromatography of the crude mixture contained some Ru(OEP)(NO)(OEt) impurity, identified by Ru-bound ethoxy peaks at −2.73 (2H, q, $J = 6.8$ Hz) and −3.07 (3H, t, $J = 6.8$ Hz) ppm in the ^{1}H-NMR spectrum. To convert all of the material to **4**, a CH_2Cl_2 solution (∼10 mL) of the mixture was stirred overnight in the dark with an equal volume of dilute sulfuric acid (0.2 M), washed first with saturated aqueous $NaHCO_3$ and then with deionized water, and dried over $MgSO_4$ and the solvent was removed *in vacuo*. A 200 mg portion of Ru(OEP)(CO)(EtOH) (0.283 mmol) led to the isolation of 159 mg of deep purple **3** (79% yield) and 41 mg of purple-red **4** (21% yield). Spectral data for **3**: UV/visible in CH_2Cl_2 (λ_{max}, nm (ϵ, M^{-1} cm^{-1})) 350^{sh} (3.5×10^4), 396 (1.42×10^5, Soret), 546^{sh} (6.7×10^3), 574 (7.4×10^3); IR (KBr; cm^{-1}) 1835 (vs), 1497 (s), 963 (s); ^{1}H-NMR ($CDCl_3$; δ, ppm) 10.38 (4H, s, *meso*), 4.19 (16H, m, $J = 7.5$ Hz, diastereotopic CH_2CH$_3$), 1.99 (24H, t, $J = 7.5$ Hz, CH$_2$CH_3); FAB-MS (*m/z*) 709 (1.4, parent), 664 (100, Ru(OEP)$(NO)^+$), 650 (32, Ru(OEP)$(O)^+$), 634 (38, Ru$(OEP)^+$). Spectral data for **4**: UV/visible in CH_2Cl_2 (λ_{max}, nm (ϵ, M^{-1} cm^{-1})) 346 (2.7×10^4), 392 (9.1×10^4, Soret), 538 (11.2×10^3), 572 (13.1×10^3); IR (KBr; cm^{-1}) 1806 (vs); ^{1}H-NMR ($CDCl_3$; δ, ppm) 10.34 (4H, s, *meso*), 4.16 (16H, m, $J = 7.5$ Hz, diastereotopic CH_2CH$_3$), 2.04 (24H, t, $J = 7.5$ Hz, CH$_2$CH_3); MS (*m/z*) 681 (14, parent), 664 (100, Ru(OEP)$(NO)^+$), 650 (20, Ru(OEP)$(O)^+$), 634 (72, Ru$(OEP)^+$). Optical spectra of **3** and **4** are included as figures in the Supporting Information.

Detection of N_2O. Experiments were carried out to determine the stoichiometry of N_2O formation from the reaction of NO with Ru(P)(CO) (P = OEP or TPP) both in the solid state and in solution (chlorobenzene). In a typical experiment, a solution of Ru(P)(CO) (∼10 mg) in minimal CH_2Cl_2 was added to a glass flask of known volume (∼30 mL; equipped with a Teflon valve for vacuum line connection and a silicone rubber septum for sample removal via syringe), and the CH_2Cl_2 was then removed under vacuum. For reactions with solid Ru(P)(CO), the flask was evacuated, refilled with the desired pressure of NO and argon (to 760 Torr total), and left at room temperature for at least 48 h in the dark. For solution reactions, deaerated chlorobenzene (1 mL) was added to the flask, and the solution was degassed to the point where only solvent vapor (10 Torr) remained in the head space. Nitric oxide and argon were then introduced, and the solution was stirred magnetically in the dark at room temperature for at least 15 h.

In order to protect the column from halocarbon vapors, the volatiles from the flask were transferred in three freeze−transfer−thaw cycles

(12) (a) Kadish, K. M.; Adamian, V. A.; Caemelbecke, E. V.; Tan, Z.; Tagliatesta, P.; Bianco, P.; Boschi, T.; Yi, G.-B.; Khan, M. A.; Richter-Addo, G. B. *Inorg. Chem.* **1996**, *35*, 1343−1348. (b) During the course of our studies, the crystal structure of **1** was communicated to us by George Richter-Addo of the University of Oklahoma and Karl Kadish of the University of Houston and subsequently published.[12a] The crystal structure solution of **1**, as well as difficulties in solving this structure, is in accord with the data presented by these workers.

(13) (a) Bohle, D. S.; Goodson, P. A.; Smith, B. D. *Polyhedron* **1996**, *15*, 3147−3150. (b) Yi, G.-B.; Khan, M. A.; Richter-Addo, G. B. *J. Chem. Soc. Chem. Commun.* **1996**, 2045−2046. (c) Yi, G.-B.; Khan, M. A.; Richter-Addo, G. B. *Inorg. Chem.* **1996**, *35*, 3453−3454. (d) Hodge, S. J.: Wang, L.-S.; Khan, M. A.; Young, V. G.; Richter-Addo, G. B. *J. Chem. Soc., Chem. Commun.* **1996**, 2283−2284.

(14) Sauve, A.; Groves, J. T. Reported at the 10th International Symposium on Homogeneous Catalysis, Princeton, NJ, Aug 199; Poster B56.

(15) Barley, M.; Becker, J. Y.; Domazetis, G.; Dolphin, D.; James, B. R. *Can. J. Chem.* **1983**, *61*, 2389−2396.

(T_f(PhCl) = 228 K) at 195 K (dry ice/acetone) to another flask of known volume at 77 K. After the second flask was allowed to warm to room temperature, argon (P_t = 760 Torr) was introduced. Gaseous aliquots (1.0 mL) for N_2O analysis were removed through the septum with a valve-equipped gastight syringe (Hamilton) and analyzed by GC with argon as the internal standard. A blank run in the absence of Ru(P)(CO) showed a background N_2O impurity in the NO sample, which usually measured <5% of the N_2O produced in the reaction of Ru(P)(CO) with NO. The N_2O values reported in Table 5 were corrected for this background. At least three injections were analyzed for each run, and the reported results are the averaged values. For N_2O measurements in which P(NO) at injection was estimated to be greater than 50 Torr, a weighted average of N_2O response factors versus Ar and NO was employed to determine $P(N_2O)$, since Ar and NO elute together.

Immediately following head space sampling, the porphyrin product was isolated by solvent removal under reduced pressure. It was then dissolved in $CDCl_3$, and the ^{1}H-NMR spectrum was recorded. The relative reactant and product concentrations from the reaction of Ru(OEP)(CO) with NO were determined by integration of the well-resolved *meso*-proton resonances of OEP. Several unidentified peaks, consisting of less than 10% of the porphyrin species, were also observed in this region. Quantitation of the amounts of relative species from the Ru(TPP)(CO) reaction was not possible because of the insolubility of these porphyrins.

Structure Determination. Suitable crystals were mounted on thin glass fibers with epoxy resin. Room-temperature single-crystal studies for all four compounds were carried out on a Siemens Smart CCD diffractometer equipped with a normal-focus 2.4 kW sealed-tube X-ray source (Mo Kα radiation) operating at 50 kV and 40 mA with a two-dimensional CCD detector. Unit cell dimensions were determined by a least-squares fit of reflections with $I > 10\sigma(I)$ and $10° < 2\theta < 56°$. The number of reflections used in the cell refinement is 2846 for **1**, 2509 for **2**, 4846 for **3**, and 3804 for **4**. About 1.3 hemispheres of intensity data were collected in 1321 frames for two tetragonal phases (**1** and **2**), and a full sphere of intensity data were collected in 2082 frames for two monoclinic phases (**3** and **4**). ω scans were used in all cases with a scan width of 0.3° and an exposure time of 30 s per frame. The empirical absorption correction was based on the symmetry-equivalent reflections, and other possible effects such as crystal decay and absorption by the glass fiber were simultaneously corrected. Crystal structures were solved by Patterson methods followed by difference Fourier methods. Computations were performed using SHELXTL running on a Silicon Graphics Indy 5000. Detailed crystal data for the four structures described here are listed in Tables 1 and 2.

(i) Complex 1. Purple crystals of **1** were grown in air at room temperature by slow vapor diffusion of Et_2O into a CH_2Cl_2 solution stored in the dark. The systematic absences observed in the reduced data for **1** were consistent with the $I\bar{4}$, $I4/m$, and $I4$ space groups. However, attempts to refine the structure in the noncentric $I4$ space group did not reveal ordering of the NO and ONO groups. Thus, the final refinement was done in the $I4/m$ space group. The NO and ONO groups are statistically distributed on two sides of the mirror plane. It is notable that several other TPP nitrosyl complexes, including Co(TPP)(NO)[16] and Fe(TPP)(NO),[17] crystallize in an 8-fold disordered manner, which leads to the choice of $I4/m$ over $I4$ as the preferred space group.[16−20] Final full-matrix refinements were performed against F^2 and included anisotropic thermal parameters for non-hydrogen atoms except those in the NO and ONO ligands. The hydrogen atoms were calculated using a C−H distance of 0.93 Å and were refined isotropically. The positional parameters of the hydrogen atoms were refined as riding parameters of their parent atoms. The maximum and minimum residual electron densities were 0.458 and −0.372 e Å^{-3}.

(ii) Complex 2. Deep red crystals of **2** were grown in air at room temperature by slow evaporation of a CH_2Cl_2/EtOH (3:1 v/v) solution protected from room light. The systematic absences were consistent with the $I\bar{4}$, $I4/m$, and $I4$ space groups. The initial structure refinement was done in the $I4$ space group, which did not show any evidence of ordering of the NO and OH groups. Thus, in the final refinement, the centric space group $I4/m$ was chosen. The NO and OH groups are statistically distributed on two sides of the mirror plane. Final full-matrix refinements were performed against F^2 and included anisotropic thermal parameters for non-hydrogen atoms except those in the NO and OH groups. The hydrogen atoms were calculated using a C−H bond distance of 0.93 Å and were refined isotropically. The positional parameters of the hydrogen atoms were refined as riding parameters of their parent atoms. The hydrogen atom of the OH group was not located. The maximum and minimum residual electron densities were 0.382 and −0.318 e Å^{-3}.

Table 1. Crystallographic Parameters for Ru(TPP)(NO)(ONO) (**1**) and Ru(TPP)(NO)(OH) (**2**)[a]

	1	**2**
empirical formula	$C_{44}H_{28}N_6O_3Ru$	$C_{44}H_{29}N_5O_2Ru$
fw	789.79	760.79
color	purple	dark red
habit	bipyramidal	plate
crystal size (mm^3)	0.17 × 0.15 × 0.067	0.17 × 0.12 × 0.067
crystal system	tetragonal	tetragonal
space group	$I4/m$ (No. 87)	$I4/m$ (No. 87)
a (Å)	13.6529(6)	13.5423(4)
c (Å)	9.7904(5)	9.7150(4)
V (Å^3)	1825.0(2)	1781.7(1)
Z (molecules/cell)	2	2
T (°C)	20	20
ρ_{calc} (g cm^{-3})	1.437	1.418
λ(Mo Kα) (Å)	0.710 73	0.710 73
μ(Mo Kα) (mm^{-1})	0.480	0.486
hkl data limits	$-18 < h < 17$, $-18 < k < 17$, $11 < l < 12$	$-18 < h < 17$, $-18 < k < 15$, $-11 < l < 12$
max 2θ (deg)	50	50
no. of total data	4845	4795
no. of unique data	855	838
$R_{int}(I)$ (%)	4.35	4.42
no. of obsd data, $I > 2\sigma(I)$	838	811
no. of parameters	86	83
R^b (%)	4.87	3.92
R_w (%)	14.05[c]	9.22
GOF	1.304	1.282

[a] The numbers in parentheses for all crystallographic tables are standard deviations. [b] $R(F) = \sum||F_o| - |F_c||/\sum|F_o|$ with $F_o > 4.0\sigma(F)$. [c] $R_w(F^2) = [\sum w(F_o^2 - F_c^2)^2/\sum w(F_o^2)^2]^{0.5}$ with $F_o > 4.0\sigma(F)$. $w = 1/[\sigma^2(F_o^2) + (AP)^2 + B]$. $P = (F_o^2 + 2F_c^2)/3$; $A = 0.046$, $B = 6.2657$ for **1**; $A = 0.0197$, $B = 4.9725$ for **2**.

(iii) Complex 3. Dark brown crystals of **3** were grown in the dark by allowing Et_2O to diffuse slowly into an aerated CH_2Cl_2 solution at room temperature. The space group was determined to be $P2_1$ from the systematic absences and intensity statistics and was confirmed by the successful structure solution. Final full-matrix refinements were performed against F^2 for all reflections and included anisotropic thermal parameters for non-hydrogen atoms. Hydrogen atoms were calculated at ideal locations and were included in the structure factor calculation as riding atoms. Parameter shifts in the final least-squares cycle were smaller than 0.03σ. The maximum and minimum residual electron densities were 0.835 and −0.546 e Å^{-3}. A methylene chloride solvent molecule was discovered within the crystal.

(iv) Complex 4. Deep purple crystals of **4** were grown by slow evaporation in air of a CH_2Cl_2/EtOH (3:1 v/v) solution stored at room temperature and in the dark. The space group, $P2_1$, was determined from the systematic absences and intensity statistics and was confirmed by the successful structure solution. An ethanol solvent molecule was discovered within the crystal. The large thermal parameters of this solvent molecule suggest that it has large thermal motions. The distance from the hydroxyl oxygen atom to the oxygen atom of the ethanol molecule is 2.53 Å, suggesting the existence of hydrogen bonding. Final

(16) Scheidt, W. R.; Hoard, J. L. *J. Am. Chem. Soc.* **1973**, *95*, 8281−8288.
(17) Scheidt, W. R.; Frisse, M. E. *J. Am. Chem. Soc.* **1975**, *97*, 17−21.
(18) Hoard, J. L.; Cohen, G. H.; Glick, M. D. *J. Am. Chem. Soc.* **1967**, *89*, 1992−1996.
(19) Glick, M. D.; Cohen, G. H.; Hoard, J. L. *J. Am. Chem. Soc.* **1967**, *89*, 1996−1998.
(20) Timkovich, R.; Tulinsky, A. *J. Am. Chem. Soc.* **1969**, *91*, 4430−4432.

Table 2. Crystallographic Parameters for Ru(OEP)(NO)(ONO) (**3**) and Ru(OEP)(NO)(OH) (**4**)

	3	**4**
empirical formula	$C_{37}H_{46}N_6O_3RuCl_2$	$C_{38}H_{51}N_5O_3Ru$
fw	794.79	726.91
color	black	dark brown
habit	plate	plate
crystal size (mm^3)	0.27 × 0.10 × 0.017	0.5 × 0.167 × 0.033
crystal system	monoclinic	monoclinic
space group	$P2_1$ (No. 4)	$P2_1$ (No. 4)
a (Å)	10.7687(2)	10.8474(7)
b (Å)	21.0320(2)	21.002(1)
c (Å)	8.5936(2)	8.3646(5)
β (deg)	102.683(1)	103.571(1)
V (Å^3)	1898.85(6)	1852.4(2)
Z (molecules/cell)	2	2
T (°C)	20	20
ρ_{calc} (g cm^{-3})	1.390	1.303
λ(Mo Kα) (Å)	0.710 73	0.710 73
μ(Mo Kα) (mm^{-1})	0.597	0.465
hkl data limits	$-14 < h < 14$, $-28 < k < 28$, $-11 < l < 11$	$-14 < h < 14$, $-27 < k < 27$, $-10 < l < 11$
max 2θ (deg)	50	45
no. of total data	15 530	12 230
no. of unique data	6579	4796
$R_{int}(I)$ (%)	7.02	7.94
no. of obsd data, $I > 2\sigma(I)$	4702	3527
no. of parameters	453	421
R^a (%)	6.23	6.74
R_w (%)	9.81[b]	13.84
GOF	1.023	1.033

[a] $R(F) = \sum||F_o| - |F_c||/\sum|F_o|$ with $F_o > 4.0\sigma(F)$. [b] $R_w(F^2) = [\sum w(F_o^2 - F_c^2)^2/\sum w(F_o^2)^2]^{0.5}$ with $F_o > 4.0\sigma(F)$. $w = 1/[\sigma^2(F_o^2) + (AP)^2 + B]$. $P = (F_o^2 + 2F_c^2)/3$, $A = 0.036$, $B = 0.0837$ for **3**, $A = 0.0745$, $B = 0.00$ for **4**.

full-matrix refinements were performed against F^2 and included anisotropic thermal parameters for all non-hydrogen atoms except those of the solvent ethanol molecule, which was refined isotropically. Hydrogen atoms, except that of the hydroxyl group, were calculated at ideal locations. The positional parameters of hydrogen atoms were refined as riding parameters of their parent atoms. Two common isotropic thermal parameters for hydrogen atoms (one for those in the methylene groups of the OEP complex and one for those on planar C atoms) were refined. Parameter shifts in the final least-squares cycle were smaller than 0.03σ. The maximum and minimum residual electron densities were 0.738 and −0.864 e Å^{-3}.

Results and Discussion

Synthesis of Ru(TPP) Nitrosyl Complexes. Reaction of a CH_2Cl_2 suspension of Ru(TPP)(CO)(EtOH) with excess NO resulted in complete loss of the carbonyl ν_{CO} band at 1945 cm^{-1} in the IR spectrum and in the appearance of new bands consistent with the ν_{NO} expected for complexes of linear nitrosyls (i.e., NO^+).[21] Column chromatography of the reaction solution led to isolation of two products. One species (**1**) displayed a ν_{NO} IR band at 1854 cm^{-1} (KBr) and two other new bands at 1522 and 930 cm^{-1}. The IR spectrum of the second compound (**2**) displayed a single ν_{NO} band at 1827 cm^{-1} (KBr). The remaining IR bands of both **1** and **2** could be attributed to the Ru(TPP) moiety and were only minimally affected by the nature of the axial ligands. The ratio of the isolated products was (apparently) dependent upon the time of NO exposure, the solvent medium, and the experimental workup, but both products were formed even from the reaction of solid Ru(TPP)(CO) and gaseous NO. In CH_2Cl_2, longer exposure times to NO strongly favored production of **1** (after isolation and crystallization as described in the Experimental Section); however, when ethanol was present, **2** was the principal product even after lengthy (30 min) reaction times. Both species appeared to be diamagnetic, given the well-resolved ^{1}H-NMR spectra having normal proton line widths (see Experimental Section).

Characterization of 1. Two structures for **1** come to mind. The first is a dinitrosyl complex, Ru(TPP)$(NO)_2$, with one axial ligand linearly bound as NO^+ and the other in the bent configuration as NO^-. The second is the nitrosyl nitrito complex Ru(TPP)$(NO^+)(ONO^-)$ with a linear nitrosyl and an O-coordinated nitrite in the axial sites. The 1522 cm^{-1} band observed for **1** lies at the lower limit of the ν_{NO} range reported for coordinated nitroxyl anions, NO^- (i.e., a bent M−N═O, >1500 cm^{-1}),[21a] yet just above the normal range for the asymmetric stretch, ν_{as}, of coordinated nitrito anions (1505−1370 cm^{-1}).[21] The new band at 930 cm^{-1} is consistent with a symmetric ONO^- stretch, ν_s, although again somewhat outside the normal range (1130−965 cm^{-1}). Previous reports of dinitrosyl metalloporphyrin complexes include the product described for the reaction of Ru(mesoporphyrin IX dimethyl ester)(CO) with NO to give a Ru(P)$(NO)_2$ species with ν_{NO} at 1838 and 1786 cm^{-1} in KBr.[9] Also reported were the reversible reaction of Fe(TPP)(NO) with NO to give Fe(TPP)$(NO)_2$ with ν_{NO} =1870 and 1690 cm^{-1} in Nujol[22] and the reaction of Os(OEP)(CO)(py) with NO to give Os(OEP)$(NO)_2$ with ν_{NO} = 1778 and 1500 cm^{-1} in KBr.[23] Structural data were not given for any of these complexes although a parent peak of *m*/*z* 755 was seen in the mass spectrum of Ru(mesoporphyrin IX dimethyl ester)$(NO)_2$.[9] The structure has been reported for a related ruthenium complex, [*trans*-Ru(sal$_2$en)(NO)(ONO)]·THF (sal$_2$en = *N*,*N*′-ethylenebis(salicylideneaminato)), formed by reaction of Ru(sal$_2$en)$(PPh_3)_2$ with NO in THF.[24] This clearly shows a nitrito ligand *trans* to the linear nitrosyl, and the IR spectrum displays a ν_{NO} band at 1831 cm^{-1} and a ν_{as}(ONO) band at 1507 cm^{-1} (KBr). Thus, the IR spectrum of **1** appears to be more consistent with a nitrosyl nitrito species rather than with a dinitrosyl complex.

Although subsequent studies, especially those of the OEP analog described below, clearly support this conclusion, initial attempts to differentiate the two possible structures were ambiguous. The FAB mass spectrum did not give a parent peak; the highest mass and most intense peak was seen at *m*/*z* 744 (Ru(TPP)$(NO)^+$). Furthermore, there was considerable disorder at the ONO^- (or NO^-) site in the X-ray crystal structure, which left open the possibility of a Ru(TPP)$(NO^+)(NO^-)$ structural assignment. However after re-examination according to a Ru(TPP)(NO)(ONO) model (see below), the refinement proved to be better. While this issue was still in question, the low-temperature (−60 °C) X-ray crystal structure of the same compound was resolved as Ru(TPP)(NO)(ONO) by Kadish, Tagliatesta, Richter-Addo, and co-workers and personally communicated to us.[12] During the same period, Bohle *et al*. also communicated to us their X-ray crystal structure solution for the closely related Ru(TTP)(NO)(ONO) (TTP = tetratolylporphyrinato dianion) complex synthesized by metathesis of Ru(TTP)(NO)Cl with $AgNO_2$.[13a]

Synthesis of Ru(OEP) Nitrosyl Complexes. Owing to the ambiguities regarding the nature of **1**, we also prepared the Ru-

(21) (a) Nakamoto, K. *Infrared Spectra of Inorganic and Coordination Compounds*, 4th ed.; John Wiley & Sons: New York, 1986. (b) Hitchman, M. A.; Rowbottom, G. L. *Coord. Chem. Rev.* **1982**, *42*, 55−132.

(22) Wayland, B. B.; Olson, L. W. *J. Am. Chem. Soc.* **1974**, *96*, 6037−6041.

(23) Buchler, J. W.; Smith, P. D. *Chem. Ber.* **1976**, *109*, 1465.

(24) Carrondo, M. A. A. F. d. T.; Rudolf, P. R.; Skapski, A. C.; Thornback, J. R.; Wilkinson, G. *Inorg. Chim. Acta* **1977**, *24*, L95.

Table 3. Electronic Spectral Data for **1**−**4** and Their Carbonyl Precursors in CH_2Cl_2 at Ambient Temperature

compd	λ_{max}, nm (log ϵ)			
		Soret band	Q(1,0)	Q(0,0)
Ru(TPP)(NO)(ONO) (**1**)	333 (4.31)	410 (5.32)	564 (4.01)	608^{sh} (3.65)
Ru(TPP)(NO)(OH) (**2**)	320 (4.30)	410 (5.14), 428^{sh}	556 (4.28)	592 (3.83)
Ru(TPP)(CO)(EtOH)	345 (3.95)	411 (5.41)	528 (4.40)	560^{sh} (3.48)
Ru(OEP)(NO)(ONO) (**3**)	350^{sh} (4.54)	396 (5.15)	546^{sh} (3.83)	574 (3.87)
Ru(OEP)(NO)(OH) (**4**)	346 (4.44)	392 (4.97)	538 (4.05)	572 (4.12)
Ru(OEP)(CO)(EtOH)	344 (4.13)	392 (5.34)	514 (4.20)	547 (4.56)

(OEP) analog by reaction of Ru(OEP)(CO)(EtOH) in CH_2Cl_2 with excess NO to give a product solution again displaying two IR bands in the ν_{NO} region. Chromatography of this solution led to isolation of two products; the major species was **3** with a ν_{NO} IR band at 1827 cm^{-1} (KBr) plus other new bands at 1497, 963, and 821 cm^{-1}, and a lesser product was **4** with a ν_{NO} band at 1806 cm^{-1} (KBr). Other IR bands could be attributed to the Ru(OEP) moiety and were minimally affected by the nature of the axial ligands. Bubbling NO through a solution of Ru(OEP)(CO) in neat CH_2Cl_2 for times as short as 5 min resulted in production of **3** in yields >70%, while in CH_2Cl_2/EtOH, **4** was the major product (>90%) even after a 30 min entrainment with NO.

Characterization of 3. The IR spectrum of **3** is quite similar to that of **1.** The ν_{NO} band at 1827 cm^{-1} is typical of a linear M−NO;[21a] the bands at 1497 and 963 cm^{-1} fall within the normal range for ν_{as} and ν_s, respectively, for coordinated ONO^-. Additionally, the band at 821 cm^{-1} corresponds to the ONO^- bending mode (850−810 cm^{-1}).[21] Furthermore, the FAB mass spectrum gave a peak at *m*/*z* 709 corresponding to the Ru(OEP)(NO)$(ONO)^+$ parent peak for **3**, although its intensity was less than 2% that of the peak at *m*/*z* 664, which corresponds to Ru(OEP)$(NO)^+$. Finally, the X-ray crystal structure of **3** was resolved in the $P2_1$ space group, which gave much less disorder at the axial ligand sites (although *R* values were higher owing to disorder of the OEP ethyl groups and the presence of a solvent of crystallization within the lattice) and clearly demonstrated the presence of both a linear nitrosyl ligand and an O-coordinated nitrito ligand (see below).

Characterization of 2 and 4. The IR spectra of compounds **2** and **4** display only single new bands at 1827 and 1806 cm^{-1}, respectively, consistent with linearly coordinated mononitrosyls. Given the normal line widths of the ^{1}H-NMR spectra, both products were concluded to be diamagnetic and therefore are Ru(II) complexes, i.e., $Ru^{II}(P)(NO^+)(X^-)$. In analogy to **1**, the highest observable molecular weight ion in the mass spectrum of **2** was Ru(TPP)$(NO)^+$. The highest *m*/*z* peak and subsequent fragmentation pattern were in accord with formulation of **4** as Ru(OEP)(NO)(OH). The OH^- ligand was unexpected, as both compounds were recrystallized from CH_2Cl_2/EtOH, so the sixth ligand was anticipated to be OEt^-. The ^{1}H-NMR spectrum was also consistent with formulation of **4** as a hydroxo complex, since ethoxy resonances (which should have occurred several ppm upfield from TMS, given ring current effects from the porphyrin ring) were not seen in spectra of the isolated product.[10] The apparent source of the OH^- is atmospheric moisture, as the recrystallization was carried out under ambient conditions. The crystal structures described below confirmed formulation of both **2** and **4** as the hydroxo species Ru(P)(NO)(OH).

Spectra. The electronic absorption spectral data for **1**−**4** in CH_2Cl_2 are presented in Table 3. These spectra exhibit a shift from the *hypso* pattern of Ru(P)(CO) to a more *normal* pattern upon NO substitution to give Ru(P)(NO)(X).[25] For *hypso* metalloporphyrins, the Q bands (ligand centered a_{1u}, $a_{2u}(\pi) \rightarrow e_g(\pi^*)$ transitions) shift to shorter wavelength because mixing of filled $e_g(d_\pi)$ metal orbitals with the empty $e_g(\pi^*)$ porphyrin orbitals moves the $e_g(\pi^*)$ orbitals to higher energy. The stronger π-accepting properties of NO^+ (relative to CO) apparently lower metal d-orbital energies, which in turn decreases the interaction with the $e_g(\pi^*)$ orbitals and results in a bathochromic shift of the Q bands. The identity of the various axial ligands X of the nitrosyl complexes Ru(P)(NO)(X) has a lesser effect on the positions of the Q and Soret bands (Table 3). This behavior is in accord with the spectra for the series Ru(TPP)(CO)(L), L = vacant < EtOH < Me_2SO < py < pip, where it was shown that the identity of L affects the intensity ratio of the Soret and Q bands but has only a modest effect on the positions of the Soret, Q(1,0), and Q(0,0) band maxima.[26]

Table 4. Effect of the *Trans* Ligand on ν_{NO} Values for Ru(P)(NO)(X) Complexes

X$^-$	ν_{NO} (P = TPP)		ν_{NO} (P = OEP)	
	in KBr	in CH_2Cl_2 (ϵ)[a]	in KBr	in CH_2Cl_2 (ϵ)[a]
OMe^- [b]			1780	
OEt^- [c]	1816		1794	
OH^- [d]	1827	1825 (1200)	1806	1814 (1300)
Cl^-			1827	1844 (1300)
ONO^-	1854	1860 (1400)	1835	1851 (1350)

[a] Extinction coefficient in M^{-1} cm^{-1}. [b] Reference 10. [c] Recrystallized in 3:1 CH_2Cl_2/EtOH under argon. [d] Recrystallized in air.

The nitrosyl stretching frequencies are listed in Table 4 for various $Ru^{II}(P)(NO)(X)$ complexes. It is noted that, owing to the strong π-back-bonding interactions between the metal and NO, the ν_{NO} for the linear nitrosyl is sensitive both to the nature of the porphyrin and to the identity of the axial ligand *trans* to it. For example, ν_{NO} is systematically +20 cm^{-1} higher for complexes of TPP than for the OEP analogs. In addition, ν_{NO} shifts to lower frequency for more basic X^-.

Thermal and Photochemical Stability. In the dark, **2** and **4** are stable in the solid phase or as solutions in noncoordinating solvents for months. In contrast, solid samples of Ru(P)(NO)(ONO) proved unstable and underwent slow conversion to the respective Ru(P)(NO)(OH) after several weeks unless stored under inert atmosphere. This reaction was significantly faster in solution, especially when not protected from room light. In coordinating solvents such as pyridine, all four compounds were slowly converted to $Ru(P)(L)_2$ over a period of days. These reactions were accelerated photochemically. In aerated solution, **1**−**4** exhibited photochemical activity upon irradiation with 366 nm light. The UV/visible spectral changes observed upon photolysis varied in different solvents, which included benzene, benzene/EtOH, CH_2Cl_2, and pyridine. However, for a particular porphyrin, the nitrito and hydroxy complexes were photolyzed to common products. For example, in CH_2Cl_2, the photolysis of **3** or **4** gave Ru(OEP)(NO)Cl as the major photoproduct, as shown by IR, UV/visible, and ^{1}H-NMR spectra and by

(25) (a) Gouterman, M. In *The Porphyrins*; Dolphin, D., Ed.; Academic: New York, 1978; Vol. III, Chapter 1. (b) Buchler, J. W. In *Porphyrins and Metalloporphyrins*; Smith, K. M., Ed.; Elsevier Scientific Publishing Co.: Amsterdam, 1975. (c) The electronic absorption spectra of metalloporphyrins generally exhibit three bands originating from $\pi \rightarrow \pi^*$ transitions. Interactions with metal d electrons can perturb these bands as well as cause the appearance of additional bands. The higher energy band (380−450 nm), termed the Soret band, is the origin B(0,0) of the second excited singlet state and is extremely intense ((1−5) × 10^5 M^{-1} cm^{-1}). The intensities of the two visible-range Q bands are about an order of magnitude lower than the Soret intensity, and these bands are found between 500 and 700 nm with a separation of approximately 1250 cm^{-1}. The Q(0,0) band is the electronic origin of the lowest energy $^1\pi\pi^*$ state, while the Q(1,0) band includes one mode of vibrational excitation.

(26) Levine, L. M. A.; Holten, D. *J. Phys. Chem.* **1988**, *92*, 714.

Table 5. Results of N_2O Detection Experiments[a]

starting material (μmol)		product (%)				yield of N_2O	
Ru(OEP)(CO)	NO	Ru(OEP)(CO)[e]	**4**[f]	**3**	other[g]	μmol	%[h]
8.5[b]	36	23	8	58	11	4.5	69
12.0[b]	36	51	2	41	6	3.9	66
12.3[b]	36	49	3	42	6	4.3	69
18.4[b]	153	0	21	71	8	13.1	70
10.8[c]	36	30	9	57	4	6.3	83
12.6[c]	50	0	38	62	<2	10.2	81
54.3[c]	310	0	10	85	5	47.8	88
19.5[c]	190	0	73	26	1	12.6	64

[a] All reactions were carried out for at least 15 h in the dark at 22 ± 3 °C. [b] Solid state. [c] In chlorobenzene (1 mL). [d] In 3:1 chlorobenzene/ethanol (1 mL). [e] Observable by ^{1}H-NMR. [f] Includes Ru(OEP)(NO)(OEt). [g] Unknown compound characterized by ^{1}H-NMR *meso*-proton peak at 10.43 ppm in $CDCl_3$. [h] Based on Ru(OEP)(CO) consumed.

comparison to an independently prepared sample.[27] A minor primary photoproduct with high ν_{NO} (>1850 cm^{-1} in CH_2Cl_2) and ^{1}H-NMR values (*meso*-proton resonances at 10.43 ppm) was also observed, which has yet to be identified. The photochemical properties of these materials will be reported elsewhere.[8]

Stoichiometry of the Reaction of NO with Ru(OEP)(CO). The reactions leading to the Ru(II) nitrosyl products of the synthesis scheme are not straight forward. Formally, both Ru(P)(NO)(OH) and Ru(P)(NO)(ONO) are in the Ru(II) oxidation state, as are the carbonyl analogs. However, at least formally, the nitric oxide has undergone oxidation to N(III) both for coordinated NO^+ and for ONO^-. Since the metal is not reduced, the likely oxidant in deaerated media is nitric oxide itself. In this context, experiments to identify the reduced nitrogen product and to evaluate the reaction stoichiometries were initiated to provide a more complete perspective regarding the chemical transformations leading to the above products.

The dependence of the product ratio on synthetic conditions initially suggested that Ru(P)(NO)(ONO) may be formed in some manner by direct reaction of NO with Ru(P)(NO)(OR). To evaluate this suggestion, a solution of **2** in CH_2Cl_2 was exposed to NO for 30 min. After solvent removal under vacuum, the IR spectrum of the solid had three new bands at 1845, 1517, and 930 cm^{-1} and the nitrosyl stretch characteristic of **2** had a much reduced intensity. Thus, incomplete conversion of **2** into **1** had occurred as the result of exposure to NO. However, this observation proved to be misleading. Subsequent experiments were carried out where rigorous efforts were made to ensure that dioxygen impurities were not present in a solution of Ru(OEP)(NO)(OR) and that the NO gas added was free of other nitrogen oxide impurities. Under such conditions, there was very little conversion into Ru(OEP)(NO)(ONO); thus, the conversion of the alkoxy or hydroxy complex to the nitrito analog appears to involve reaction with the strong nitrosating agents formed during NO autoxidation.[28]

Nonetheless, when the reaction of Ru(OEP)(CO) with NO was carried out under rigorously deoxygenated conditions, the nitrito complex still proved to be the major product in the solid phase or in noncoordinating solvents. This implies the operation of a mechanism independent of Ru(OEP)(NO)(OR) formation or NO autoxidation by adventitious dioxygen. In order to further probe the nature of this reaction, the gaseous products of the reaction of Ru(OEP)(CO) with NO were examined by GC and mass spectral analysis, and both CO and N_2O were identified. Owing to interference from the NO signal, the amount of CO released could not be quantified, but since there was no evidence of CO_2 formation, it will be assumed that CO was not oxidized during the synthetic sequence. As described in the Experimental Section, quantitative experiments were carried out to determine (by ^{1}H-NMR) the amount of Ru(OEP)(CO) consumed and the amounts of Ru(OEP)(NO)(ONO) and Ru(OEP)(NO)(OR) formed.

Scheme 1. Hypothetical Intermediates Enroute to Formation of the Nitrosyl Nitrito Complexes

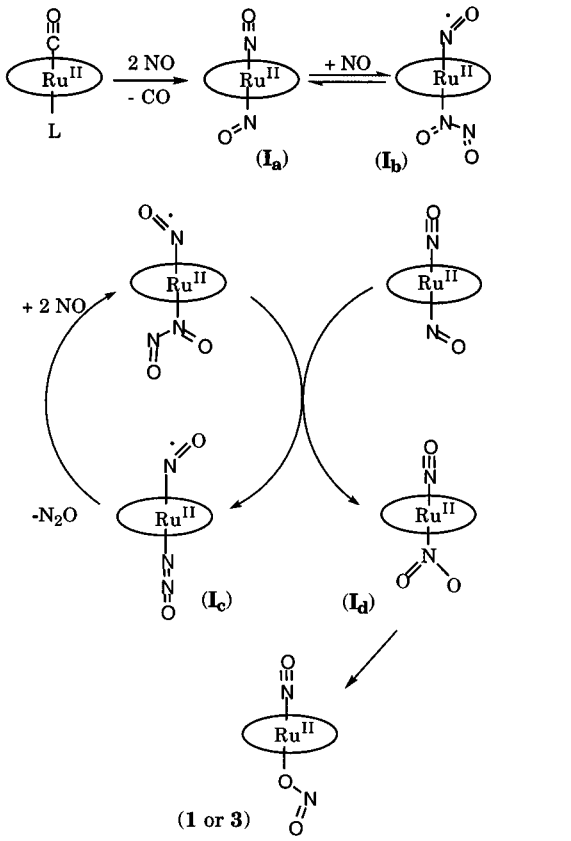

Table 6. Atomic Coordinates (× 10^4) and Equivalent Isotropic Displacement Parameters (Å^2 × 10^3) for Ru(TPP)(NO)(ONO) (**1**)

atom	*x*	*y*	*z*	U_{eq}[a]
Ru(1)	0	0	0	48(1)
N(1)	−1444(4)	−401(4)	0	56(1)
C(1)	−1802(5)	−1345(5)	0	60(2)
C(2)	−2844(5)	−1297(6)	0	67(2)
C(3)	−3098(6)	−355(6)	0	70(2)
C(4)	−2236(5)	226(5)	0	59(2)
C(5)	−1241(5)	−2188(5)	0	60(2)
C(6)	−1789(5)	−3139(5)	0	64(2)
C(7)	−2048(6)	−3591(5)	−1190(9)	100(2)
C(8)	−2572(6)	−4455(5)	−1181(10)	111(3)
C(9)	−2834(7)	−4878(7)	0	97(3)
N(2)	0	0	1760(18)	113(19)
O(1)	0	0	2899(21)	97(6)
O(2)	0	0	1939(16)	50(6)
N(3)	498(28)	−285(36)	2806(28)	82(12)
O(3)	0	0	3777(42)	198(15)

[a] The equivalent isotropic thermal parameter, U_{eq}, is defined as one-third of the trace of the orthogonalized $\mathbf{U}_{ij}$ tensor.

(27) According to the procedure of Bohle et al.,[13] a stirred CH_2Cl_2 solution of **3** was treated with gaseous HCl for 5 min, during which the solution darkened to a color similar to that of **4**. Solvent removal afforded a dark purple crystalline solid. Spectral data: UV/visible in CH_2Cl_2 (λ_{max}, nm (ϵ/10^3, M^{-1} cm^{-1})) 354 (31), 399 (140, Soret), 467^{sh} (8.8), 547^{sh} (6.6), 568 (6.8); IR (CH_2Cl_2, KBr) 1844 (1300 M^{-1} cm^{-1}), 1827 cm^{-1}; ^{1}H-NMR ($CDCl_3$; δ, ppm) 10.39 (s, 4H, *meso*), 4.19 (m, diastereotopic CH_2CH_3, 16H, J = 7.5 Hz), 2.01 (t, CH_2CH_3, 24H, J = 7.5 Hz); FAB-MS *m*/*z* 699 (parent), 669 (Ru(OEP)(Cl)$^+$), 664 (Ru(OEP)(NO)$^+$), 634 (Ru(OEP)$^+$).

(28) Ford, P. C.; Wink, D. A.; Stanbury, D. M. *FEBS Lett.* **1993**, *326*, 1−3.

Table 7. Selected Bond Lengths and Angles for Ru(TPP)(NO)(ONO) (**1**)

Bond Distances (Å)			
Ru(1)−N(1)	2.047(5)	N(2)−O(1)	1.12(2)
Ru(1)−N(2)	1.72(2)	O(2)−N(3)	1.16(2)
Ru(1)−O(2)	1.90(2)	O(3)−N(3)	1.23(2)
N(1)−C(1)	1.378(9)	C(2)−C(3)	1.332(11)
N(1)−C(4)	1.379(9)	C(3)−C(4)	1.419(10)
C(1)−C(2)	1.424(10)	C(5)−C(6)	1.499(10)
Bond Angles (deg)			
N(1)−Ru(1)−N(1)	180.0	O(2)−N(3)−O(3)	108.0(30)
N(1)−Ru(1)−N(1)	90.0	Ru(1)−O(2)−N(3)	137.3(18)
N(1)−Ru(1)−N(2)	90.0	Ru(1)−N(2)−O(1)	180.0
N(1)−Ru(1)−O(2)	90.0	N(2)−Ru(1)−O(2)	180.0
Ru(1)−N(1)−C(1)	126.3(5)	N(1)−C(1)−C(2)	108.1(6)
N(1)−C(1)−C(5)	125.6(6)	C(1)−C(2)−C(3)	107.7(7)
C(2)−C(3)−C(4)	108.9(7)	C(3)−C(4)−N(1)	107.7(6)
C(1)−C(5)−C(6)	116.4(6)	C(5)−C(6)−C(7)	121.4(4)

Table 8. Atomic coordinates ($\times 10^4$) and equivalent isotropic displacement parameters (Å^2 $\times$ 10^3) for Ru(TPP)(NO)(OH) (**2**)

atom	*x*	*y*	*z*	U_{eq}[a]
Ru(1)	0	0	0	34(1)
N(1)	−376(3)	1466(3)	0	38(1)
C(1)	−1328(4)	1844(4)	0	41(1)
C(2)	−1257(4)	2908(4)	0	48(1)
C(3)	−300(4)	3144(4)	0	51(1)
C(4)	266(4)	2256(4)	0	41(1)
C(5)	−2194(3)	1294(4)	0	41(1)
C(6)	−3148(4)	859(4)	0	42(1)
C(7)	−3592(3)	2129(4)	1194(5)	80(2)
C(8)	−4466(4)	2665(4)	1193(6)	90(2)
C(9)	−4891(4)	2930(4)	0	66(2)
N(2)	0	0	1777(9)	91(14)
O(1)	0	0	2990(11)	74(4)
O(2)	0	0	−1928(12)	22(4)

[a] The equivalent isotropic thermal parameter, U_{eq}, is defined as one-third of the trace of the orthogonalized $\mathbf{U}_{ij}$ tensor.

Table 9. Selected Bond Lengths and Angles for Ru(TPP)(NO)(OH) (**2**)

Bond Distance (Å)			
Ru(1)−N(1)	2.050(4)	Ru(1)−O(2)	1.873(11)
Ru(1)−N(2)	1.726(9)	N(2)−O(1)	1.179(9)
N(1)−C(1)	1.387(6)	C(2)−C(3)	1.334(7)
N(1)−C(4)	1.377(6)	C(3)−C(4)	1.427(7)
C(1)−C(2)	1.443(7)	C(5)−C(6)	1.502(7)
Bond Angles (deg)			
N(1)−Ru(1)−N(1)	180.0	N(2)−Ru(1)−O(2)	180.0
N(1)−Ru(1)−N(1)	90.0	N(1)−Ru(1)−O(2)	90.0
N(1)−Ru(1)−N(2)	90.0	Ru(1)−N(2)−O(1)	180.0
Ru(1)−N(1)−C(1)	126.0(3)	N(1)−C(1)−C(2)	107.8(4)
N(1)−C(1)−C(5)	126.0(5)	C(1)−C(2)−C(3)	107.7(5)
C(2)−C(3)−C(4)	108.6(5)	C(3)−C(4)−N(1)	108.4(4)
C(1)−C(5)−C(6)	117.0(4)	C(5)−C(6)−C(7)	121.2(3)

For the same reactions, the N_2O formation was quantified by GC analysis. These data are summarized in Table 5.

A balanced equation (eq 1) for the direct formation of Ru(OEP)(NO)(ONO) from the reaction of Ru(OEP)(CO) with NO

$$\text{Ru(OEP)(CO)} + 4\text{NO} \rightarrow \text{Ru(OEP)(NO)(ONO)} + \text{CO} + \text{N}_2\text{O} \quad (1)$$

suggests a 1:1 stoichiometry for the formation of N_2O and **3.** This is based on the assumptions that NO is the only oxidant in the reaction (rather than O_2 or other nitrogen oxides) and that N_2O is the only nitrogen oxide product other than those still coordinated to Ru.

Two pathways with different stoichiometries can be envisioned for the formation of **4**. For example, the reaction of Ru(OEP)(CO) with NO might give **3** directly followed by alcoholysis or hydrolysis of this species to give **4** (eq 2). In

$$\text{Ru(OEP)(NO)(ONO)} + \text{HOR} \rightarrow \text{Ru(OEP)(NO)(OR)} + \text{NO}_2^- + \text{H}^+ \quad (2)$$

this case, the stoichiometry of N_2O formation would be the same as that for formation of **3** (eq 1), i.e., 1:1.

Alternatively, **4** could be formed directly by a redox pathway with NO (e.g., eq 3). In that case, a 1:2 stoichiometry for the

$$2\text{Ru(OEP)(CO)} + 4\text{NO} + 2\text{HOR} \rightarrow 2\text{Ru(OEP)(NO)(OR)} + \text{H}_2\text{O} + \text{N}_2\text{O} + 2\text{CO} \quad (3)$$

formation of N_2O and **4** would be predicted, since reaction of **4** with NO does not lead to **3** directly unless other oxidants are present.

Table 10. Atomic Coordinates ($\times 10^4$) and Equivalent Isotropic Displacement Parameters (Å^2 $\times$ 10^3) for Ru(OEP)(NO)(ONO) (**3**)

atom	*x*	*y*	*z*	U_{eq}[a]
Ru(1)	1600(1)	25(1)	1301(1)	37(1)
N(1)	247(4)	−187(2)	2597(7)	32(2)
N(2)	877(6)	−669(3)	−339(9)	36(2)
N(3)	3088(4)	156(3)	191(6)	34(2)
N(4)	2452(6)	645(3)	3067(9)	32(2)
C(1)	−912(6)	−1013(3)	819(9)	37(2)
C(2)	2408(6)	−591(3)	−2028(9)	37(2)
C(3)	4244(6)	956(3)	1959(9)	37(2)
C(4)	936(6)	536(3)	4813(9)	38(2)
C(11)	122(5)	87(5)	3987(8)	33(2)
C(12)	−980(6)	−176(3)	4482(9)	37(2)
C(13)	−1492(7)	−626(3)	3373(9)	40(2)
C(14)	−715(6)	−635(3)	2173(9)	35(2)
C(21)	−175(8)	−1036(4)	−321(10)	33(2)
C(22)	−406(7)	−1456(3)	−1678(8)	37(2)
C(23)	518(7)	−1332(3)	−2493(8)	38(2)
C(24)	1337(7)	−843(3)	−1638(8)	35(2)
C(31)	3223(6)	−134(3)	−1179(9)	36(2)
C(32)	4358(6)	108(5)	−1630(8)	35(2)
C(33)	4869(7)	556(3)	−518(9)	37(2)
C(34)	4073(6)	582(3)	617(9)	32(2)
C(41)	3557(7)	991(3)	3129(10)	34(2)
C(42)	3798(7)	1383(4)	4562(11)	37(2)
C(43)	2857(7)	1254(3)	5353(8)	37(2)
C(44)	2015(6)	795(3)	4405(8)	31(2)
C(15)	−1421(5)	35(6)	5925(7)	44(2)
C(16)	−2115(7)	674(4)	5703(10)	64(3)
C(17)	−2643(6)	−1031(4)	3351(9)	50(2)
C(18)	−3901(7)	−719(4)	2665(11)	68(3)
C(25)	−1465(7)	−1939(3)	−2076(9)	47(2)
C(26)	−1140(9)	−2578(4)	−1326(12)	87(3)
C(27)	732(7)	−1653(4)	−4000(10)	53(2)
C(28)	1637(9)	−2209(6)	−3725(11)	84(4)
C(35)	4864(6)	−125(4)	−2995(9)	51(3)
C(36)	5613(8)	−738(4)	−2669(11)	70(3)
C(37)	6013(6)	958(4)	−478(10)	46(2)
C(38)	7225(7)	702(5)	558(11)	85(3)
C(45)	4920(7)	1820(3)	5022(9)	47(2)
C(46)	4667(8)	2474(4)	4329(12)	79(3)
C(47)	2675(6)	1555(3)	6855(9)	43(2)
C(48)	1671(9)	2088(5)	6571(12)	73(4)
N(5)	705(7)	635(3)	182(9)	38(2)
N(6)	2704(9)	−810(4)	3793(11)	82(3)
O(1)	178(7)	1038(4)	−661(9)	82(2)
O(2)	2688(6)	−670(3)	2419(7)	48(2)
O(3)	3344(7)	−1250(4)	4341(10)	79(2)
Cl(1)	4671(6)	−2245(2)	354(6)	192(2)
Cl(2)	2342(4)	−2583(2)	1323(7)	199(2)
C(5)	3414(19)	−2005(6)	933(16)	194(9)

[a] The equivalent isotropic thermal parameter, U_{eq}, is defined as one-third of the trace of the orthogonalized $\mathbf{U}_{ij}$ tensor.

Table 11. Selected Bond Lengths (Å) and Angles (deg) for Ru(OEP)(NO)(ONO) (**3**)

Bond Distance (Å)			
Ru(1)−N(1)	2.067(5)	N(5)−O(1)	1.177(9)
Ru(1)−N(2)	2.059(7)	N(6)−O(2)	1.214(10)
Ru(1)−N(3)	2.056(5)	N(6)−O(3)	1.188(9)
Ru(1)−N(4)	2.058(7)	Cl(1)−C(5)	1.63(2)
Ru(1)−N(5)	1.758(7)	Cl(2)−C(5)	1.76(2)
Ru(1)−O(2)	1.984(6)		

Bond Angles (deg)			
N(1)−Ru(1)−N(2)	90.6(2)	Ru(1)−N(1)−C(11)	126.9(4)
N(1)−Ru(1)−N(3)	172.9(2)	Ru(1)−N(1)−C(14)	125.3(4)
N(2)−Ru(1)−N(3)	89.6(2)	Ru(1)−N(2)−C(21)	125.4(6)
N(1)−Ru(1)−N(4)	89.9(7)	Ru(1)−N(2)−C(24)	126.8(5)
N(2)Ru(1)−N(4)	173.9(3)	Ru(1)−N(3)−C(31)	125.7(4)
N(3)−Ru(1)−N(4)	89.4(2)	Ru(1)−N(3)−C(34)	126.7(5)
N(1)−Ru(1)−N(5)	94.9(3)	Ru(1)−N(4)−C(41)	127.0(6)
N(2)Ru(1)−N(5)	93.6(2)	Ru(1)−N(4)−C(44)	125.7(5)
N(3)−Ru(1)−N(5)	92.2(3)	Ru(1)−N(5)−O(1)	174.0(8)
N(4)−Ru(1)−N(5)	92.5(3)	O(2)−N(6)−O(3)	117.3(9)
N(1)−Ru(1)−O(2)	89.6(2)	Ru(1)−O(2)−N(6)	122.0(6)
N(2)−Ru(1)−O(2)	84.5(3)	N(5)−Ru(1)−O(2)	175.2(3)
N(3)−Ru(1)−O(2)	83.4(2)	Cl(1)−C(5)−Cl(2)	117.4(7)
N(4)−Ru(1)−O(2)	89.4(2)		

If other oxidants, such as adventitious O_2, participated, the ratio would be lower than 1:2. Thus, rationalization of the nitrito complex **3** via initial formation of **4** would require that the maximum stoichiometry of N_2O formation in that case not be greater than 0.5.

As can be seen in Table 5, the molar ratio of N_2O detected to Ru(OEP)(CO) consumed ranged from 0.68 to 0.88, which, despite the care taken to transfer all volatiles from the solution to the sampling flask, should be regarded as lower limits. Thus, the observed $\Delta N_2O/\Delta$Ru(OEP)(CO) ratios exceeding 0.5 support the view that **3** is formed in a direct manner (eq 1) and not by the intermediate formation of **4** followed by nitrosation of this species by NO autoxidation intermediates. On the other hand, these data do not allow one to clearly determine whether **4** is formed via a "direct" pathway such as eq 3 or by the initial formation of **3** followed by the hydrolysis or alcoholysis to give **4** (eqs 1 and 2). If both species were formed by initial formation of **3**, the predicted ratio would be 1:1, and the values reported in Table 5 thus may simply reflect inefficiency in N_2O transfer and analysis. Alternatively, if **3** and **4** are formed by independent direct pathways as in eqs 1 and 3, the $\Delta N_2O/\Delta$Ru(OEP)(CO) ratio will depend on the relative quantities of these two products formed in the competitive pathways. On the basis of this model, the N_2O values in Table 5 would represent 73−102% yields of the theoretical values.

Metal complexes have long been known to promote the disproportionation of NO.[29,30] Scheme 1 is a proposed reaction sequence for the formation of the nitrito complexes **1** and **3** without invoking the intermediacy of **2** and **4**, respectively. The key steps are the coordination of NO first to labilize the CO and then to form the putative dinitrosyl complex (**I$_a$**). Electrophilic attack of free NO on the bent Ru−NO moiety would give a Ru{N(O)NO} species (**I$_b$**) from which oxygen atom transfer to a second equivalent of (**I$_a$**) gives a nitrous oxide complex (**I$_c$**) plus a nitro (N-bound NO_2) complex (**I$_d$**). Loss of N_2O from **I$_c$** and reaction with another equivalent of NO would regenerate **I$_a$**. Simple linkage isomerization of **I$_d$** would give the Ru(P)(NO)(ONO) species **1** (P = TPP) or **3** (P = OEP).

Table 12. Atomic Coordinates ($\times 10^4$) and Equivalent Isotropic Displacement Parameters ($Å^2 \times 10^3$) for Ru(OEP)(NO)(OH) (**4**)

atom	*x*	*y*	*z*	U_{eq}[a]
Ru(1)	8232(1)	9958(1)	8663(1)	40(1)
N(1)	9612(7)	10153(3)	7404(9)	30(2)
N(2)	8961(10)	10661(5)	10338(14)	37(3)
N(3)	6770(8)	9833(6)	9818(10)	45(3)
N(4)	7421(11)	9307(5)	6891(15)	36(3)
C(1)	10758(9)	10977(5)	9188(13)	37(3)
C(2)	7462(10)	10567(5)	12107(14)	44(3)
C(3)	5622(10)	8983(6)	8004(13)	46(3)
C(4)	8903(11)	9411(5)	5140(13)	43(3)
C(11)	9713(9)	9851(6)	6007(13)	32(3)
C(12)	10825(9)	10121(5)	5470(12)	41(4)
C(13)	11346(10)	10568(5)	6621(14)	38(3)
C(14)	10567(10)	10584(5)	7827(13)	35(3)
C(21)	10076(11)	11021(6)	10380(17)	41(3)
C(22)	10269(10)	11451(4)	11773(13)	37(3)
C(23)	9339(10)	11337(5)	12604(13)	43(3)
C(24)	8540(11)	10824(6)	11695(14)	47(3)
C(31)	6642(10)	10068(11)	11222(15)	58(6)
C(32)	5540(9)	9843(6)	11703(12)	37(3)
C(33)	5048(10)	9393(6)	10585(14)	44(3)
C(34)	5808(10)	9372(5)	9374(15)	44(3)
C(41)	6396(10)	8946(5)	6832(12)	31(3)
C(42)	6118(10)	8548(5)	5417(14)	45(3)
C(43)	7022(10)	8687(5)	4555(12)	36(3)
C(44)	7839(10)	9137(5)	5527(13)	36(3)
C(15)	11276(9)	9917(9)	4010(11)	54(3)
C(16)	11933(12)	9264(6)	4259(17)	75(4)
C(17)	12480(10)	10980(5)	6629(14)	46(3)
C(18)	13718(12)	10675(7)	7455(18)	96(5)
C(25)	11311(12)	11916(5)	12183(15)	59(3)
C(26)	11013(14)	12559(7)	11406(19)	90(5)
C(27)	9098(12)	11656(6)	14128(16)	61(3)
C(28)	8268(17)	12214(10)	13759(22)	125(10)
C(35)	5047(11)	10078(8)	13134(13)	61(5)
C(36)	4312(13)	10699(6)	12833(19)	73(4)
C(37)	3891(11)	8953(6)	10533(14)	54(3)
C(38)	2627(11)	9233(7)	9532(18)	88(5)
C(45)	5042(11)	8065(5)	4951(14)	53(3)
C(46)	5326(13)	7431(6)	5745(22)	104(6)
C(47)	7228(11)	8376(5)	3022(14)	53(3)
C(48)	8233(14)	7852(8)	3355(18)	79(6)
N(5)	9107(12)	9373(5)	9860(15)	38(3)
O(1)	9617(10)	8941(5)	10578(14)	85(4)
O(2)	7181(10)	10609(4)	7324(15)	55(3)
O(3)	7177(26)	11816(12)	7359(34)	306(12)
C(5)	7330(27)	12238(14)	8765(36)	239(14)
C(6)	6094(25)	12030(14)	9288(35)	235(13)

[a] The equivalent isotropic thermal parameter, U_{eq}, is defined as one-third of the trace of the orthogonalized $\mathbf{U}_{ij}$ tensor.

The nitrous oxide complex **I$_c$** finds precedence in the pentaammineruthenium(II) species $Ru(NH_3)_5(N_2O)^{2+}$ reported by Armor and Taube.[31]

An alternative scheme (not depicted) for formation of the nitrosyl nitrito product would be one in which **I$_a$** or **I$_b$** is oxidized by oxygen atom transfer from the simple dimer ON−NO to give **I$_d$** plus N_2O directly. This would give the same stoichiometry (1:1) as eq 1.

As noted above, there have been several literature reports of dinitrosyl metalloporphyrin complexes that are analogous to **I$_a$** although structural studies are lacking. In this context, it is notable that the reaction of a toluene solution of Co(TPP)(NO) with NO initially produced the paramagnetic compound Co(TPP)$(NO)_2$.[32] An increase in the pressure of NO above 20 Torr resulted in reversible formation of a diamagnetic compound believed to be the result of the addition of a third nitrosyl ligand to form Co(TPP)(NO)(N_2O_2). Some analogy can also be seen

(29) (a) Bottomley, F. Reactions of Nitrosyls. In *Reactions of Coordinated Ligands*; Braerman, P. S., Ed.; Plenum Press: New York, 1989; Vol. 2. (b) McLeverty, J. A. *Chem. Rev.* **1979**, *79*, 53.
(30) Gwost, D.; Caulton, K. G. *Inorg. Chem.* **1974**, *13*, 414−417.
(31) Armor, J. N.; Taube. H. *J. Am. Chem. Soc.* **1969**, *91*, 6874−6876.
(32) Wayland, B. B; Minkiewicz, J. V. *J. Chem. Soc., Chem. Commun.* **1976**, 1015−1016.

Table 13. Selected Bond Lengths and Angles for Ru(OEP)(NO)(OH) (**4**)

	Bond Distance (Å)		
Ru(1)−N(1)	2.063(7)	Ru(1)−N(5)	1.723(11)
Ru(1)−N(2)	2.061(11)	Ru(1)−O(2)	1.956(11)
Ru(1)−N(3)	2.059(8)	N(5)−O(1)	1.155(14)
Ru(1)−N(4)	2.056(12)	O(3)−C(5)	1.452(14)
	Bond Angles (deg)		
N(1)−Ru(1)−N(2)	89.8(3)	N(4)−Ru(1)−O(2)	87.6(3)
N(1)−Ru(1)−N(3)	174.9(4)	N(5)−Ru(1)−O(2)	177.8(5)
N(2)−Ru(1)−N(3)	89.3(4)	Ru(1)−N(1)−C(11)	124.2(7)
N(1)−Ru(1)−N(4)	90.2(3)	Ru(1)−N(1)−C(14)	126.8(6)
N(2)−Ru(1)−N(4)	175.8(5)	Ru(1)−N(2)−C(21)	125.9(9)
N(3)−Ru(1)−N(4)	90.4(4)	Ru(1)−N(2)−C(24)	126.6(9)
N(1)−Ru(1)−N(5)	94.1(4)	Ru(1)−N(3)−C(31)	128.9(9)
N(2)−Ru(1)−N(5)	92.6(4)	Ru(1)−N(3)−C(34)	124.7(7)
N(3)−Ru(1)−N(5)	90.9(5)	Ru(1)−N(4)−C(41)	128.0(9)
N(4)−Ru(1)−N(5)	91.6(6)	Ru(1)−N(4)−C(44)	127.2(8)
N(1)−Ru(1)−O(2)	88.0(3)	Ru(1)−N(5)−O(1)	173.7(12)
N(2)−Ru(1)−O(2)	88.2(5)	O(3)−C(5)−C(6)	96.5(22)
N(3)−Ru(1)−O(2)	87.0(4)		

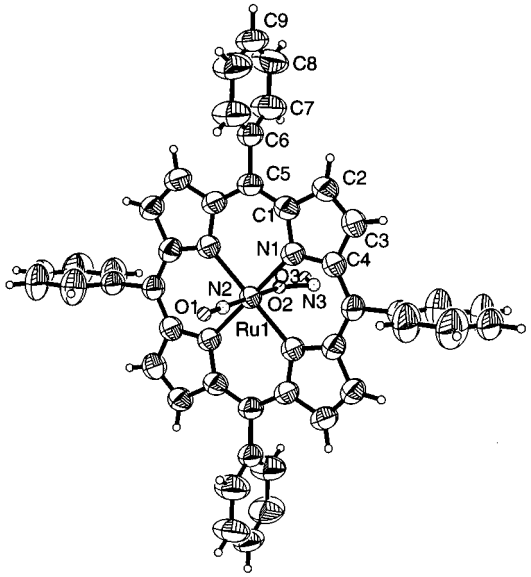

Figure 1. Molecular structure and numbering of atoms for Ru(TPP)(NO)(ONO) (**1**). Hydrogen atoms are omitted for clarity. Thermal ellipsoids are drawn at the 50% level.

in the reaction of $[Fe(TPP)]_2O$ with excess NO in deaerated toluene solution to give the nitrosyl nitro complex Fe(TPP)(NO)(NO_2).[33] The overall stoichiometry of the reaction was proposed to be that shown in eq 4, although gaseous products were not analyzed.

$$[Fe(TPP)]_2O + 6NO \rightarrow 2Fe(TPP)(NO)(NO_2) + N_2O \quad (4)$$

X-ray Crystal Structures. Cell parameters and details of the data collection and final refinement are summarized for **1** and **2** in Table 1 and for **3** and **4** in Table 2. The atomic coordinates and equivalent isotropic thermal parameters, U_{eq}, are listed in Tables 6−9 and selected bond distances and angles are given in Tables 10−13, for **1**−**4**, respectively. The structures are depicted in Figures 1−4. The ellipsoids in these figures, which depict each atom, are consistent with the equivalent isotropic and anisotropic thermal parameters.

Comparisons of Structures. All four compounds have linear or nearly linear nitrosyl ligands. However, the perfect linearity (180°) of the TPP complexes may be a result of the symmetry restriction. The replacement of the ONO^- group by the smaller

(33) Settin, M. F.; Fanning, J. C. *Inorg. Chem.* **1988**, *27*, 1431−1435.

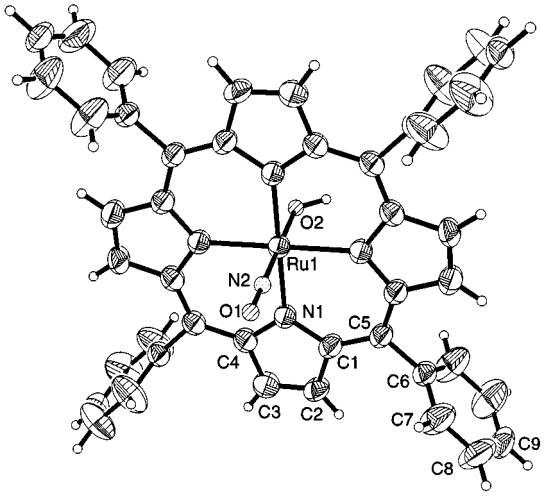

Figure 2. Molecular structure and numbering of atoms for Ru(TPP)(NO)(OH) (**2**). Hydrogen atoms are omitted for clarity. Thermal ellipsoids are drawn at the 50% level.

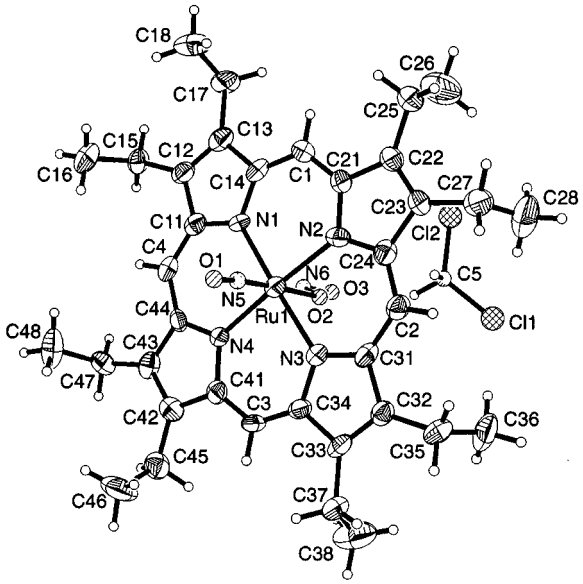

Figure 3. Molecular structure and numbering of atoms for Ru(OEP)(NO)(ONO) (**3**). Hydrogen atoms are omitted for clarity. Thermal ellipsoids are drawn at the 50% level.

OH^- group in the TPP complexes leads a unit cell contraction in all three axial directions. However, this is not seen for the two OEP complexes, as the sizes and orientations of solvent molecules also have a sizable effect. As expected from the molecular symmetry of these complexes, the OEP complexes crystallize in a lower space group symmetry than the corresponding TPP complexes. The size of the central ruthenium cation matches the size of the hole in the center of the porphyrin ring; thus neither ruffling of the porphyrin ring nor lifting (or lowering) of the ruthenium center above (or below) the ring plane is observable in any of the four complexes.

It should be noted that, for the structures reported here, the substituents on the porphyrin rings dictate the crystal packing mode, so whether one of the axial ligands is ONO^- or OH^- has negligible effect. In order to achieve efficient packing, the larger phenyl rings and ethyl groups apparently have precedence over the smaller axial ligands.

The crystal structures of **1** and **2** are nearly the same except in the identity of the ligand *trans* to NO, consistent with the similar spectroscopies of these two compounds. The 8-fold disorder in the axial positions for these structures compromises

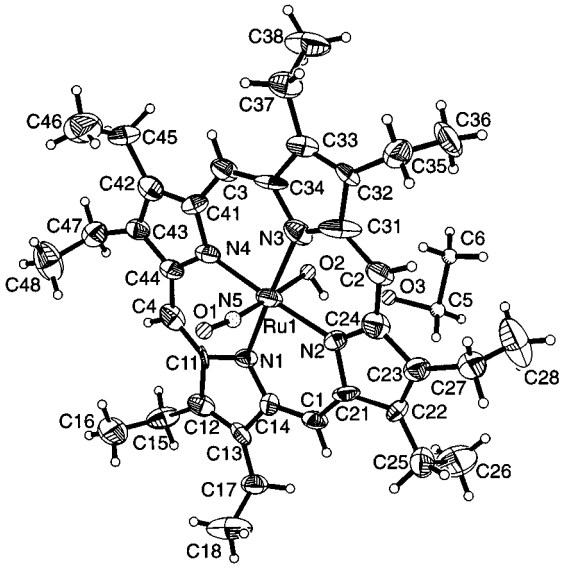

Figure 4. Molecular structure and numbering of atoms for Ru(OEP)(NO)(OH) (**4**). Hydrogen atoms are omitted for clarity. Thermal ellipsoids are drawn at the 50% level.

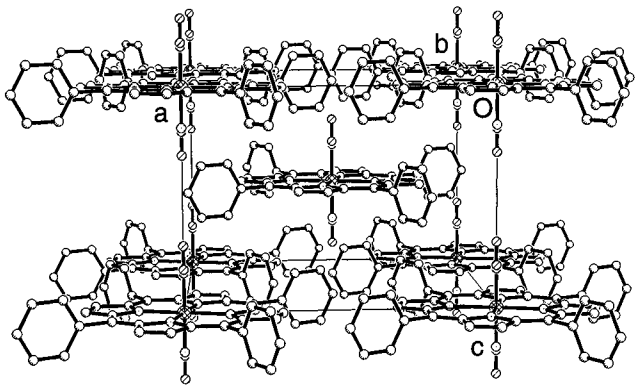

Figure 5. Unit cell packing diagram for Ru(TPP)(NO)(OH) (**2**) showing columns of molecules stacked along the *c* axis.

the accuracy of the bond distances and angles at these locations, so quantitative comparison of these data are of limited value. The two TPP complexes have nearly identical packing diagrams; that for the hydroxyl species is shown here (Figure 5). In both complexes, the center of the porphyrin ring (i.e., the location of the Ru cation) is at the unit cell origin, which has a point group symmetry of *I*4/*m*. Such a point group symmetry is consistent with the molecular symmetry of the TPP molecule. The molecules are stacked into parallel columns along the tetragonal *c* axis. The axial ligands apparently do not generate adequate intermolecular interactions to force molecules to align in a single direction. This leads to the crystallographic disorder involving the statistical distribution of the nitrosyl and its *trans* ligand.

Such a lack of interaction and the associated disorder can also be understood from the overall packing of the molecules. When the TPP complexes are stacked into columns, a large void space surrounding the nitrosyl group and the ligand *trans* to it is generated. The perpendicular distance between two porphyrin planes along the chain corresponds to the *c* axial length, which is as long as 9.7 Å in the hydroxyl phase (the distance between two porphyrin planes is half of the *c* axis, 4.85 Å, if the molecule at the unit cell body center is considered). Such a large void space might be reduced by moving two porphyrin rings more closely together, which might lead to alignments, but this is apparently prevented by steric interactions between the phenyl rings. Instead, the void space is mostly filled with the phenyl

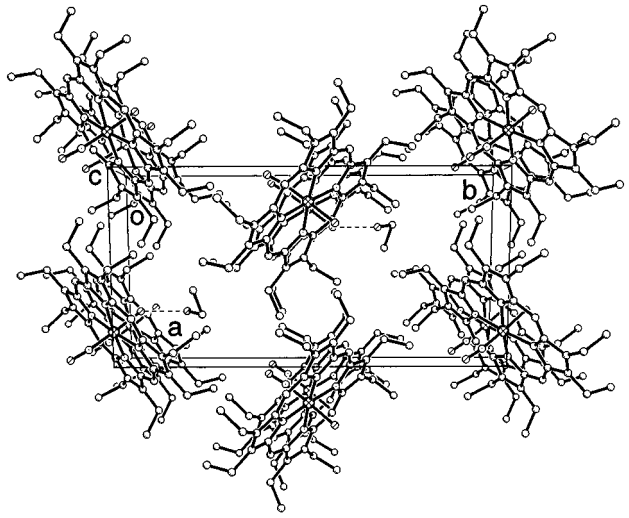

Figure 6. Unit cell packing diagram for Ru(OEP)(NO)(OH) (**4**) showing three sheets of OEP complexes stacked along the *b* axis. The dashed line represents the hydrogen bonding between the hydroxyl group and the ethanol molecule.

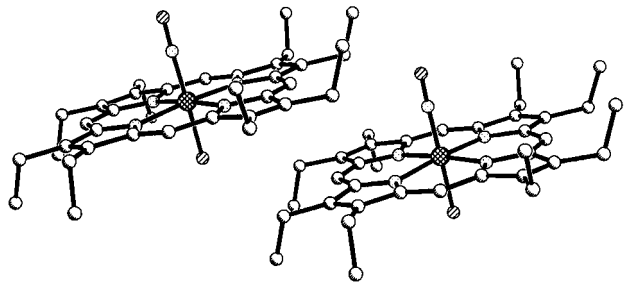

Figure 7. Two molecules of Ru(OEP)(NO)(OH) (**4**) showing the relative offset of porphyrin centers and conformation of ethyl groups.

rings located at the unit cell body center (Figure 5), which produces an efficient packing mode. This may also explain the absence of solvent molecules in the TPP complexes.

The disorder present in **1** and **2** presents difficulties in unambiguously determining the nature of axial ligands on the ruthenium center. To some extent, this issue was resolved by preparing the OEP complexes, which have lower crystallographic symmetry and thus do not have structural disorder at the axial sites. The structures of **3** and **4** are similar in nearly all parameters except for the identities of the ligand *trans* to NO and of the solvent molecules within the crystal lattices. The two OEP complexes have nearly identical packing modes; the packing diagram for the hydroxyl phase is shown here (Figure 6). The crystal structure consists of sheets of OEP complexes stacked along the crystallographic *b* axis with solvent molecules located in the cavities between the sheets. Within each sheet, all porphyrin planes have the same orientation; however, porphyrin planes in two adjacent sheets are oriented perpendicular to each other (Figure 6). For **4**, the shortest perpendicular distance between two porphyrin planes of two OEP complexes is 3.67 Å. This is more than 1 Å shorter than the corresponding distance in the TPP complexes. The shorter distance in OEP complexes can be explained by the flexible conformation of the ethyl groups, which remain on one side of the porphyrin ring near the region of overlap (Figure 7). In contrast, the phenyl ring is perpendicular to the porphyrin ring in the TPP complexes and protrudes above and below the porphyrin ring.

The conformation of the ethyl groups is an important feature of compounds **3** and **4** and affects the overall packing of molecules. The two ethyl groups on the same pyrrole ring are

on the same side of the porphyrin ring. Four adjacent ethyl groups are on the same side, while the other four adjacent ethyl groups are on the opposite side. Such a conformation is the same as that in a recently synthesized Fe(OEP) compound[33] but differs from that in a Co(OEP) complex.[34]

Summary. The reaction of nitric oxide with the ruthenium carbonyls Ru(P)(CO) (P = TPP, OEP) leads to the formation of the nitrosyl complexes Ru(P)(NO)(OH) and Ru(P)(NO)(ONO). Nitrous oxide is also formed in this reaction, and it is proposed that the reaction proceeds via the formation of the Ru(II) dinitrosyl intermediate $Ru(P)(NO)_2$, which is oxidized by oxygen atom transfer from either free or Ru-coordinated N_2O_2. The crystal structures of all four complexes have been determined. The structural features of these compounds are in agreement with the spectroscopic results. A comparison of these structures shows that the crystal packing modes are determined to a large extent by the peripheral substituents on the porphyrin rings and are relatively insensitive to the nature of the small ligands present. We can expect that the interplay between the size of porphyrin substituents and the size of relatively large axial ligands would lead to a wide variety of crystal structures whose packing modes seem to be determined by the principle of closest packing. These results represent the first systematic studies of ruthenium nitrosyl porphyrins and can serve as a useful guide for the design and characterization of new metal nitrosyl porphyrins.

Acknowledgment. This work was supported by the National Science Foundation (Grant CHE 9400919). We thank Professors Karl Kadish (University of Houston) and George Richter-Addo (University of Oklahoma) for providing a copy of ref 12 before publication and Professor D. Scott Bohle (University of Wyoming) for providing a copy of ref 13a before publication. We also are grateful to Professor Everly Fleischer (University of California, Irvine) for providing valuable advice regarding the preparation of metalloporphyrin complexes.

Supporting Information Available: Listings of complete structure refinement details, bond lengths and angles, anisotropic displacement parameters for non-hydrogen atoms, and hydrogen coordinates and isotropic displacement parameters and figures showing the electronic spectra of compounds **1**−**4** in dichloromethane (34 pages). Ordering information is given on any current masthead page.

IC970065B

(34) Senge, M. O. *Acta Crystallogr.* **1996**, *C52*, 302−305.
(35) Scheidt, W. R.; Turowska-Tyrk, I. *Inorg. Chem.* **1994**, *33*, 1314−1318.